

インテリジェント・リフレクティング・サーフェス(IRS)アンテナ向けの低損失と高速応答を備えた進歩した液晶

藤澤 宣、佐藤弘康、石川 理、陳 強、豊島 展、中谷誠和、
石鍋隆宏(正会員)、藤掛英夫(フェロー)、陳 強

要旨液晶を用いたインテリジェント反射面(IRS)の性能向上に着目して研究を行っている。1~50GHzの広い周波数範囲で同軸線を用いた液晶の誘電特性の特性評価を実現し、高いネマティック-等方性転移温度を有する3-リングまたは4-リング化合物が損失正接に対して還元効果を示すことを明らかにした。液晶を用いたIRSアンテナの応答時間と損失正接を改善するために、極性基を持たないパラ-テルフェニル液晶化合物を導入することで、40GHz帯以上の周波数で0.01に近い低損失正接と、ほぼ半分の応答減衰時間の短縮を同時に達成した。

キーワード：損失正接、比誘電率、周波数依存性、インテリジェント・リフレクティング・サーフェス、ギガヘルツ帯域

1. Introduction

液晶は、誘電率の異方性の特性から導かれる誘電率の変化によって、ギガヘルツ波やテラヘルツ波でも制御可能な伝搬であるという魅力的な物質に注目されている。電気通信における移相器やアンテナなどの液晶を使用する部品は、基礎研究からその応用まで広く研究されている¹⁾。

ガラス基板上に配列する各アンテナ素子の位相変化を調整することで、ギガヘルツ波の反射方向を制御可能な液晶を用いたインテリジェント反射面(IRS)の研究を行っている²⁾³⁾。

電気通信における液晶の研究には、高周波(RF)領域における誘電率や損失正接に伴う誘電率異方性の挙動を理解することが、部品の特性を進歩させるために不可欠である。

液晶を用いた広範な情報ディスプレイは、電気光学特性を利用して、数十Hzの低周波での誘電異方性と光学屈折率異方性に依存する。一方、電気通信機器では、RF帯域の位相変化を利用し、低周波領域⁴⁾の印加電圧で発生する液晶の再配向に位相が依存する。

IRSアンテナに使用される誘電体層としての液晶は、アンテナ素子を配置する上部基板と接地電極基板の下部基板からなる2枚の板の間に挟まれている。この構造は、液晶ディスプレイ(LCD)に類似しており、液晶は画素電極基板と接地電極の間に挟まれている。液晶との違いは、ギガヘルツ領域のアレイ上の各アンテナ素子の反射位相が、各アンテナ素子に低周波電圧を印加して発生した棒状の液晶分子の再配向によって制御されていることである。さらに、上部に形成されるアンテナ素子のパターン電極の形状と、中央部の誘電体層としての誘電率の変化から、入射電波に対するギガヘルツ領域の共振周波数が決定される⁵⁾。

前面基板上に配置されたアンテナ素子による入射波の反射方向を変化させるためには、LC誘電体層による大きな連続位相変化を達成することがIRSアンテナの本質的な機能である。

Received March 29, 2024; Revised June 12, 2024; Accepted sept 2, 2024

^{†1} Department of Communications Engineering, Graduate School of Engineering, Tohoku University (Sendai, Japan)

^{†2} Department of Electronics Engineering, Graduate School of Engineering, Tohoku University (Sendai, Japan)

^{†3} Department of Management Science and Technology, Graduate School of Engineering, Tohoku University (Sendai, Japan)

This paper includes videos. Note that the videos are not viewable from this PDF file. The videos are available as separate files on the website that hosts this PDF file.

【機械翻訳コンテンツの著作権について】

当サイトに掲載されている原著論文の著作権は映像情報メディア学会に帰属します。原著論文および翻訳論文の無断使用は禁止します。引用の際には、必ず原著論文の書誌情報をご記載ください。詳細は映像情報メディア学会著作権規定をご覧ください。

Advanced Liquid Crystals with Low Loss Tangent and Fast Response for Intelligent Reflecting Surface Antennas

Toru Fujisawa^{†1}, Hiroyasu Sato^{†1}, Wataru Ishikawa^{†2}, Hiraku Toshima^{†2},
Masakazu Nakatani^{†2}, Takahiro Ishinabe^{†3} (member),
Hideo Fujikake^{†2} (fellow) and Qiang Chen^{†1}

Abstract We are focusing our research attention on the improvement of performance for the intelligent reflecting surfaces (IRS) using liquid crystals. By realizing characterization of dielectric properties in liquid crystals using coaxial line in a wide range of frequency from 1 to 50 GHz, it is revealed that the 3-ring or 4-ring compounds possessing a high nematic-isotropic transition temperature exhibit the effects of reduction for loss tangent. For improving response time and loss tangent of IRS antenna using liquid crystals, low loss tangent reaching closely to 0.01 at frequency over 40 GHz band and shortening decay time for the response in almost half were achieved simultaneously by introducing para-terphenyl liquid crystal compounds without polar groups.

Keywords: Loss tangent, Relative permittivity, Frequency dependence, Intelligent reflecting surfaces, Gigahertz band.

1. Introduction

Liquid crystals have been paid attention to an attractive material being a controllable propagation even for gigahertz wave or terahertz wave by variation of permittivity to be derived from properties of anisotropy for permittivity. Components using liquid crystals such as phase shifter and antennas in telecommunications are extensively investigating from fundamental research to their applications¹⁾.

We have been investigating the intelligent reflecting surfaces (IRS) using liquid crystals possessing controllable reflective direction of gigahertz waves by adjusting phase change at each antenna element to be arrayed on the glass substrate²⁾³⁾.

For research of liquid crystals in the telecommunications, understanding their behavior of dielectric anisotropy associated with permittivity and loss tangent in the range of radio frequencies (RF) is

essential matters to progress the properties of the components. Widespread information displays using liquid crystals employ electro-optical properties to be depended on dielectric anisotropy on tens Hz of low frequency and optical refractive index anisotropy. On the other hand, the devices in telecommunications utilize the phase change at a RF band, where the phase depends on reorientation of liquid crystals to be occurred with an applied voltage at a low frequency range⁴⁾.

Liquid crystals as dielectric layer using to the IRS antenna are sandwiched between the two plates consisting of the top substrate arranging antenna elements and the bottom of a ground electrode substrate. This structure is similar to Liquid crystal displays (LCDs) whose liquid crystals are sandwiched between the pixel electrodes substrate and the ground electrode. The difference against LCDs is that the reflective phase on each antenna elements on the array in gigahertz region is controlled by a reorientation of rod-like shaped liquid crystalline molecules occurred with applying low- frequency voltage to each antenna element. In addition, the shape of patterned electrode of antenna elements to be formed at the top and the variation of permittivity as dielectric layer at the middle determines resonance frequency in gigahertz region against incident radio waves⁵⁾.

For altering reflection direction of incident waves by the antenna elements arranged on the front substrate, attaining a large continuous phase change by the LC

Received March 29, 2024; Revised June 12, 2024; Accepted sept 2, 2024

^{†1}Department of Communications Engineering, Graduate School of Engineering, Tohoku University (Sendai, Japan)

^{†2}Department of Electronics Engineering, Graduate School of Engineering, Tohoku University (Sendai, Japan)

^{†3}Department of Management Science and Technology, Graduate School of Engineering, Tohoku University (Sendai, Japan)

This paper includes videos. Note that the videos are not viewable from this PDF file. The videos are available as separate files on the website that hosts this PDF file.

IRSアンテナの実験結果は、アンテナ素子の電極パターンを最適に設計することで、十分な位相変化を得るために $50\mu\text{m}$ 以上の厚い誘電体層が必要であることを実証した。このような層の厚みの増加は、LC固有の特性に由来するスイッチング時間の増加により、反射方向を変化させる速度が不十分となる。また、厚いLC層を持つLC層では損失正接が増加するため、反射上の強度が減少する。

このようなアンテナの性能はLCの物理的特性と密接に関係しているため、ギガヘルツ領域におけるLCの特性向上はIRSアンテナの性能向上に重要な役割を果たす。

本論文では、ギガヘルツ帯の液晶の特性評価と、IRSアンテナに適した液晶の物性について述べる。

2. Experiment

RFの範囲における液晶の特性評価方法は、少なくともkHzの10以下の低周波の範囲における誘電率異方性の評価方法とは相容れない。その理由は、テスト対象デバイス(DUT)の線長よりも短くなる波長は、媒体間の境界で複数の反射波が発生し、定在波が発生するなど、電磁波の様々な伝搬が発生するためである。このような複雑な電界の発生を回避し、測定誤差を発生させるためには、伝送線路に沿って単一の電磁モードを伝搬するように設計された同軸線のような横電磁(TEM)伝送線路を使用する方法が効果的である。

図1にギガヘルツ帯域の測定用デバイスのブロック図を示す。セットアップは2つの関数で構成される。一つはRF信号の伝搬を測定するためのものであり、もう一つはDUTに低周波バイアス電圧を印加するためのものである。RF信号の装置は、Keysight社製のベクトルネットワークアナライザ(VNA)P5008A、液晶を誘電体層として使用するDUTの同軸ライン、低周波バイアス電圧がVNAのポートに侵入するのを防ぐためのバイアスティー(バイアスT)のペアで構成されている。その他の機器は、低周波用のファンクションジェネレーターとDCアンプで構成されている。

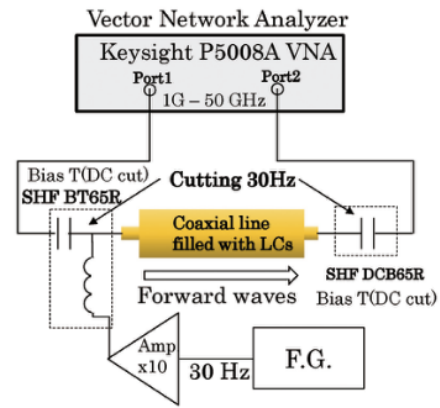


図1 DUTの誘電体層として液晶に低周波電圧を印加するためのSパラメータと配線接続を測定する装置。

これらのセットアップにより、100kHzから500Hzの周波数範囲における同軸線内の波の変化に関連するSパラメータを測定することができる。散乱行列を表すSparametersは、VNAを装備する2ポートの前方波と後方波の関係を示す。行列要素 S_{11} , S_{12} , S_{21} , S_{22} を散乱パラメータまたはSパラメータと呼ぶ。 S_{11} と S_{22} のパラメータは反射係数の意味を持ち、 S_{21} と S_{12} は透過係数の意味を持つ。測定では、DUTを介した透過波をVNAで S_{21} として検出した。LCの比誘電率と損失正接は、以下の段落で説明する抽出方法で、測定された S_{21} から抽出される。図1に示すLCで満たされた同軸線は、移動RF信号を妨害することなく、関数発生器からバイアスTを通過する低周波電圧が同軸線のLCに印加されることを特徴としている。LCのスペーサーで区切られた円筒形の内側導体と外側導体からなる同軸線の構造を利用することで、内側導体と外側導体の間に0~50Vrmsの範囲の低周波交流電圧をLCに印加することで、LCの再配向によるRFの比誘電率の異方性を測定することが可能である。

図2は、内側導体と外側導体の間に位置するポリテトラフルオロエチレン(PTFE)の一部を液晶で置き換えることができるDUT同軸線の構造を示している。図2(a)に示す通常同軸線と、図2(b)に示すLC充填部を構成するためにカスタマイズした同軸線を比較すると、PTFEを用いて誘電体層を除去した部分に中心導体が出現していること、および通常同軸線から外側導体が出現していることが確認できる。

dielectric layer is an essential function of the IRS antenna. Our experimental results of the antenna has been demonstrated that the IRS antenna requires a thick dielectric layer more than 50 μm to attain a sufficient phase change by optimal design of pattern in electrode of antenna elements. Such an increasing the thickness of layer causes an insufficient speed for altering reflective direction due to an increase of switching time derived from an inherent property of LCs. In addition, an increase of loss tangent in LC layer with a thick LC layer leads to a decrease of intensity on the reflection.

Since such performances of antenna closely relate to the physical properties of LCs, improvement of properties for LCs in the gigahertz region plays an important role to progress the performance of the IRS antenna.

In this paper, the characterization for liquid crystals in the range of gigahertz, and the physical properties in liquid crystals to be suitable for IRS antenna are described.

2. Experiment

The method for characterization of liquid crystals in the range of RF is incompatible with the method for that of dielectric anisotropy in the range of low frequencies less than ten of kHz at least. The reason is that the wavelength to be shortened than the line length of the device under test (DUT) arises various propagations of electromagnetic waves such as multiple reflected waves at boundaries between media and generation of standing waves. To avoid occurrence of such complex electric field causing errors of measurements, the method using transverse electromagnetic (TEM) transmission lines such as coaxial line, which are designed for propagating a single electromagnetic mode along the transmission line, is effective methods.

Figure 1 shows the block diagram of the device for the measurement in the range of gigahertz band. The setup is composed of two functions. One is for measurements of propagation in RF signals, and the other is for applying a low frequency bias voltage to the DUT. The equipment for RF signal is composed of a vector network analyzer (VNA) P5008A manufactured by Keysight, a coaxial line for the DUT to use liquid crystals as dielectric layer, pair of bias tees (Bias T) to prevent a low frequency bias voltage to be intruded into ports of VNA. The other equipment is composed of a function generator for the low frequency, and DC amplifier. These setups allow us to measure S-parameters associated with changes of waves within a coaxial line in

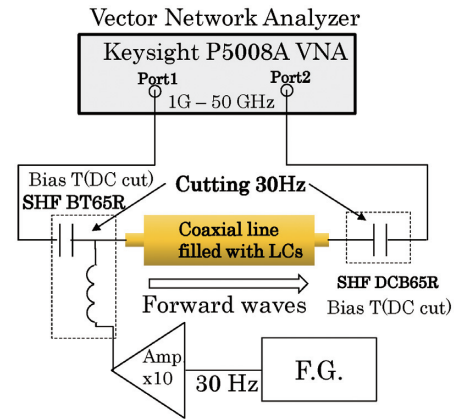


Fig. 1 Equipment to measure S-parameter and wiring connection to apply a low frequency voltage to liquid crystals as dielectric layer in DUT.

the range of frequency from 100 kHz to 50 GHz. The S-parameters representing the scattering matrix indicate the relation between the forward waves and the backward waves on the two-ports to be equipped for VNA. The matrix elements S_{11} , S_{12} , S_{21} , and S_{22} are referred to as the scattering parameters or the S-parameters. The parameters for S_{11} and S_{22} have the meaning of reflection coefficients, and S_{21} and S_{12} have the meaning of transmission coefficients. In the measurements, the transmitted waves through DUT are detected as S_{21} with VNA. The relative permittivity and loss tangent for LCs are extracted from the measured S_{21} with the method of extraction described in the following paragraphs.

The coaxial line filled with LCs shown in Figure 1 features that a low frequency voltage passing through Bias T from the function generator is applied to LCs in the coaxial line without obstructing travelling RF signal. By utilizing structure of coaxial line consisting of cylindrical inner conductors and outer conductors separated by a spacer of LCs, it is possible to measure anisotropy in the relative permittivity in RF due to reorientation of LCs by applying a low frequency AC voltage in the range from 0 to 50 Vrms between the inner conductors and the outer conductors to LCs.

Figure 2 shows the structure of DUT coaxial line that is able to replace a part of polytetrafluoroethylene (PTFE) located between the inner and the outer conductors with liquid crystals. When comparing the normal coaxial line shown in Fig.2 (a) with the customized coaxial line to build LC filling section shown in Fig. 2 (b), it is identified that the center conductor has appeared at the portion removing the dielectric layer using PTFE and the outer conductor from the normal coaxial line. This opening

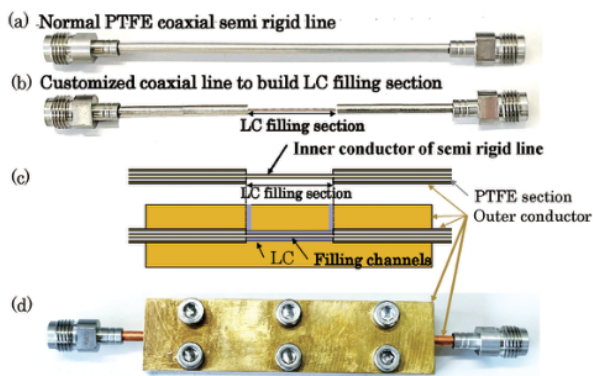


図2 同軸線の実験セットアップ。(a) 参考にPTFEを用いた同軸線、(b) 未知の液晶を用いたDUT同軸線、(c) DUTの断面図、(d) 完全DUTの概要。

この開口部はLCの充填に使用され、図2(c)に示すように、容器と外側導体の機能を持つ金属アタッチメントで覆われている。図2(c)に示すようなDUT同軸線を形成する金属付着は、図2(b)に示す開口部空間の内側導体を金属付着面上の半円筒溝に合わせるように安定に保持される。図2(d)に示す完成時のDUTは、図2(b)に示すDUTの同軸線に金属付着部の2つのピースの溝面を重ねることで、円筒形の空間を形成することができる。

実際のIRSアンテナにおけるスイッチング応答の立ち上がり時間について、1kHzのバースト矩形波印加電圧によって、アライメントが平行から垂直に遷移する際に、連続的に容量が変化することを経過時間とともに測定した。測定装置はKeysight LCR meter E4980ALで、静電容量の変化はサンプリングレート70msecで取得した。減衰時間については、垂直から平行へのアライメント遷移時に発生する静電容量の変化を測定した。

3. ギガヘルツにおけるLCの特性評価原理

比誘電率と損失正接に関する同軸線を用いた基本的な測定方法について議論する。

図3に示す S_{21} の大きさの周波数依存性は、PTFEを用いた基準とLCを充填したDUTのそれぞれについて、同軸線を通る透過波の大きさを表している。両同軸線とも、周波数が高くなるにつれて大きさが小さくなる傾向がある。LCを誘電体層として用いたDUT線は、PTFE同軸線と比較して、

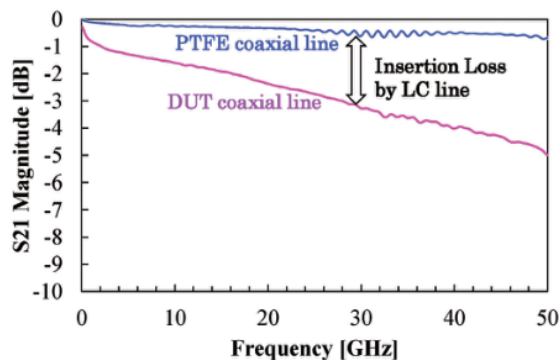


図3 各DUT線とPTFE線における S_{21} の大きさの周波数依存性の例。

周波数の関数として大きな振幅減衰を示す。DUT同軸線によるこのような大きな減衰は、LCの損失正接による挿入損失が、ギガヘルツ帯で0.002から0.005の範囲の低損失正接を持つPTFE線よりも大きいことを示唆している。

この S_{21} の大きさの減衰は、式(1)で与えられる減衰定数 α によって評価される。

$$\alpha = \frac{|S_{21}|_{dB} \ln 10}{-20 z} \quad [\text{Nepers/m}] \quad (1)$$

ここで、 z は同軸線の線長を表す。 $|S_{21}|_{dB}$ は S_{21} の大きさをdBで示す。 α はNepers/mの単位を持つ。

図4は、PTFEを用いたDUT同軸線と基準同軸線による S_{21} の位相の周波数依存性をそれぞれ示している。

図4に示すDUTと基準同軸線との位相変化の差は、PTFEを用いた基準同軸線と比較して、DUTに用いたLCの比誘電率が大きいことに起因している。相は式(2)で示されるので、比誘電率 ϵ_r は式(2)を用いて決定される。ここで、 μ_0 は真空の透磁率を表し、 ϵ_0 は次のことを表す。

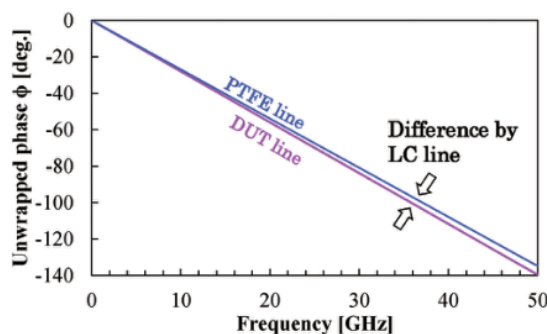


図4 DUT線とPTFE線における S_{21} の位相の周波数依存性の例。

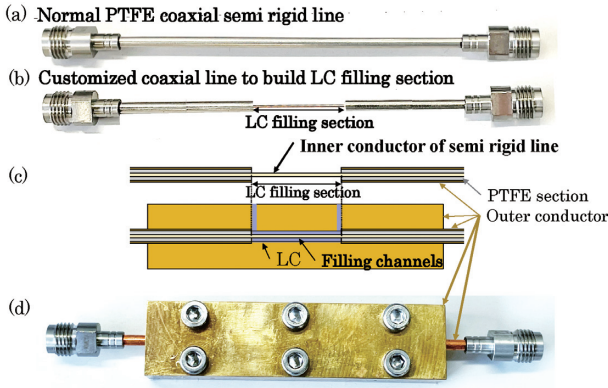


Fig.2 Experimental setup of coaxial line. (a) Coaxial line using PTFE for reference, (b) DUT coaxial line using unknown liquid crystals, (c) Cross sectional view for DUT, (d) Overview of complete DUT.

space is used for filling with LCs and is covered with the metal attachment possessing the function of the container and the outer conductor as shown in Fig. 2(c). The metal attachment to form the DUT coaxial line as shown in Fig. 2(c) holds steady to align the inner conductor of opening space shown in Fig. 2(b) with semi-cylindrical groove on the surface of metal attachment. The DUT on completion shown in Fig. 2(d) can be assembled by overlapping the groove surface of two pieces in the metal attachment to the coaxial line for the DUT shown in Fig. 2 (b) so that a cylindrical space is formed.

For the rise time in switching response in the real IRS antenna, occurring a continuous change of capacitance at the transition of alignment from a parallel to a vertical by the applied voltage of bursting square wave at 1 kHz was measured with the elapsed time. The apparatus for measurement was Keysight LCR meter E4980AL, and the change of capacitance was acquired with a 70 msec of sampling rate. For the decay time, the change of capacitance occurred at the transition of alignment from the vertical to the parallel was measured.

3. Principle of Characterization for LCs in Gigahertz

The fundamental method of measurement using coaxial line concerning relative permittivity and loss tangent is discussed.

Frequency dependence of magnitude of S_{21} shown in Fig.3 represents the magnitude of transmitted wave through coaxial line for the reference using PTFE and for the DUT filling with LCs, respectively. There is tendency that the magnitude decreases as frequency increases in both coaxial lines. The DUT line using LCs as dielectric layer exhibits a large attenuation on

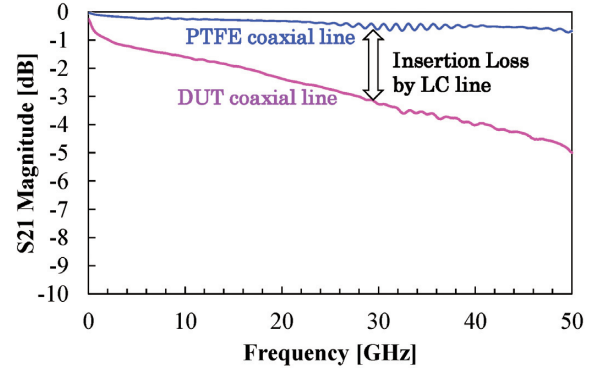


Fig.3 Example of frequency dependence of magnitude of S_{21} for each DUT line and PTFE line.

magnitude as a function of frequency in comparison with the PTFE coaxial line. Such a large attenuation by DUT coaxial line suggests that an insertion loss caused by loss tangent in LCs is larger than that of PTFE line possessing low loss tangent ranging from 0.002 to 0.005 in gigahertz band.

This attenuation for magnitude of S_{21} is evaluated by the attenuation constant α given by equation (1).

$$\alpha = \frac{|S_{21}|_{dB} \ln 10}{-20 z} \quad [\text{Nepers/m}] \quad (1)$$

where, z denotes the line length of the coaxial line. $|S_{21}|_{dB}$ indicates the magnitude of S_{21} in dB. α has units of Nepers/m.

Fig. 4 shows frequency dependence of phase in S_{21} with DUT coaxial line and reference coaxial line using PTFE, respectively.

The difference for the variation of phase between the DUT and the reference coaxial line shown in Figure 4 is caused by a large relative permittivity of LCs used to DUT in comparison with that of the reference coaxial line using PTFE. As the phase is denoted by the equation (2), the relative permittivity ϵ_r is determined by using equation (2), where μ_0 denotes the vacuum permeability, and ϵ_0 denotes

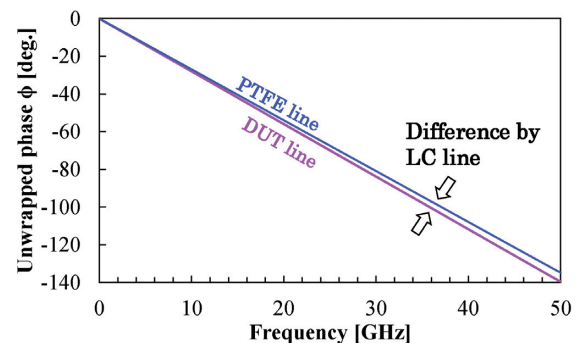


Fig.4 Example of frequency dependence of phase of S_{21} for DUT line and PTFE line.

真空の誘電率。

$$\phi = 2\pi f z \sqrt{\epsilon_r \epsilon_0 \mu_0} \quad (2)$$

位相定数 β は、同軸線に沿った単位長さあたりの移動波の位相の変化を表す。式(2)で求めた ϵ_r を式(3)に代入すると、位相定数 β が得られる。

$$\beta \approx k_0 \sqrt{\mu_0 \epsilon_r} \quad (3)$$

複素誘電率 ϵ_c は式(4)で与えられる。式(4)で与えられる ϵ_c の実部と虚部はそれぞれの式(5)と式(6)に関連しており、 ω は角周波数、 c_0 は真空中の光速である。

$$\epsilon_c = \epsilon_r' - j\epsilon_r'' \quad (4)$$

$$\epsilon_r' = -\frac{(\alpha^2 - \beta^2)c_0^2}{\omega^2} \quad (5)$$

$$\epsilon_r'' = \frac{j(2\alpha\beta)c_0^2}{\omega^2} \quad (6)$$

式(1)で与えられる α と式(3)で与えられる β を ϵ_c の実部を表す式(5)と ϵ_c の虚部を表す式(6)に代入すると、複素誘電率 ϵ_c が得られる。比誘電率 ϵ_r は ϵ_c の実数部によって決まる。

$\tan \delta$ の損失正接は、複素誘電率における ϵ_r'' と ϵ_r' の比から得られる。

4. 結果と考察

IRSアンテナにLCを適応させるためには、低周波領域やギガヘルツ領域におけるLCの物理的特性の改善が重要な課題である。

本節では、RFにおける誘電率と損失正接について議論する。低周波での交流電圧によるスイッチング応答も示している。

4.1 ギガヘルツ帯におけるLCの誘電率の周波数依存性

Sパラメータの S_{21} から求めたLCの比誘電率 ϵ_r' 、すなわち複素誘電率の実数部の周波数依存性を図5に示す。2種類の液晶混合液との誘電率の比較を図5に示す。図5のE7はよく知られた液晶である。TD1020を開発し、50 μm の厚いセルギャップでもスイッチングの減衰時間を短縮した。誘電率異方性の分類は、図5の括弧内に示されている。

DUT内のLCの配向は、無印加電圧でのランダムな配向から50Vrms印加電圧でのホメオトロピック配向への再配向で変化するので、ホメオトロピック配向における比誘電率 $\epsilon_r //$ は、DUT同軸線に50Vrms印加時の飽和状態である S_{21} の測定から得られる。

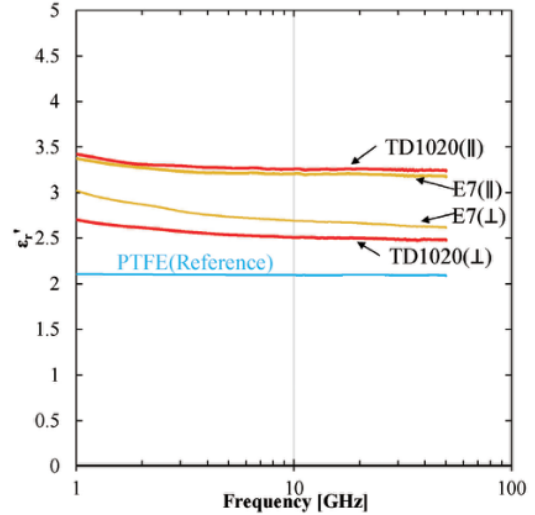


図5 誘電率異方性に対する比誘電率 ϵ_r' の周波数特性。(//)はTD1020とE7のそれぞれのLCの平行成分における ϵ_r' を表し、(*)はLCの垂直成分における ϵ_r' を表す。

DUTに電圧を印加しない場合、DUTのLCに接触する内側と外側の導体の表面に均質なアラシメント層のコーティングがないため、ランダムな配向が発生する。LCのランダムな配向における比誘電率 ϵ_{avr} は、DUT同軸線に0Vrms印加時の S_{21} の測定から得られる。誘電率異方性の垂直成分 $\epsilon_r \Delta$ は $\epsilon_r //$ と ϵ_{avr} の項を含めて式(7)で表される。

$$\epsilon_r \perp = \frac{3\epsilon_{avr} - \epsilon_r //}{2} \quad (7)$$

同軸線の基準に対するPTFEの ϵ_r' は、1GHzから50GHzの範囲では周波数にほとんど依存しないが、TD1020とE7の ϵ_r' は周波数が高くなるにつれて単調に減少する。さらに、TD1020とE7の比誘電率の誘電率異方性に基づく異なる変化が図5で観察される。

複素誘電率における損失正接、すなわち ϵ_r'' と ϵ_r' の比の周波数依存性を図6に示す。

損失正接の周波数依存性は、周波数が高くなるにつれて徐々に減少することが観察された。また、損失正接は40GHzの領域で最小となる。

これらの周波数依存性は、1GHz以下の低周波数帯域で発生した双極子緩和に由来することが示唆される。これは、周波数が高くなるにつれて双極子緩和の影響が徐々に小さくなる

the vacuum permittivity.

$$\phi = 2\pi f z \sqrt{\varepsilon_r \varepsilon_0 \mu_0} \quad (2)$$

Phase constant β represents the variation of phase in travelling wave per unit length along the coaxial line.

By substituting the ε_r determined by equation (2) into equation (3), the phase constant β is obtained.

$$\beta \approx k_0 \sqrt{\mu_0 \varepsilon_r} \quad (3)$$

The complex permittivity ε_c is given by equation (4). The real part and the imaginary part in the ε_c given by equation (4) are related to respective equation (5) and (6), where ω is the angular frequency, and c_0 is the speed of light in vacuum.

$$\varepsilon_c = \varepsilon_r' - j\varepsilon_r'' \quad (4)$$

$$\varepsilon_r' = -\frac{(\alpha^2 - \beta^2)c_0^2}{\omega^2} \quad (5)$$

$$\varepsilon_r'' = \frac{j(2\alpha\beta)c_0^2}{\omega^2} \quad (6)$$

By substituting α given by equation (1) and β given by equation (3) into equation (5) representing the real part in ε_c and equation (6) representing the imaginary part in ε_c , the complex permittivity ε_c is obtained. The relative permittivity ε_r is determined by the real part in ε_c .

The loss tangent of $\tan \delta$ is obtained from the ratio of ε_r'' to ε_r' in the complex permittivity.

4. Results and Discussion

To adapt LCs for the IRS antenna, the improvement of physical properties for LCs in the low frequency and the gigahertz regions are important issues.

In this section, the dielectric constant and the loss tangent in a RF are discussed. The switching response driven by AC voltage at a low frequency is also presented.

4.1 Frequency Dependence of permittivity for LCs in Gigahertz Band

The frequency dependence of relative permittivity ε_r' , i.e., the real part of complex permittivity for LCs determined from S_{21} of S-parameters is shown in Figure 5. The comparison of permittivity with two different liquid crystal mixtures is shown in Figure 5. E7 in Figure 5 is well-known liquid crystals. TD1020 is developed so that a decay time in switching is lowered even in a thick cell gap at 50 μ m. The classification of dielectric anisotropy is denoted inside the brackets in Figure 5.

As the orientation of LCs in the DUT is varied with reorientation from the random orientation at no applied voltage to the homeotropic orientation with applied voltage at 50 Vrms, the relative permittivity $\varepsilon_{r\parallel}$ in a homeotropic alignment is obtained from the

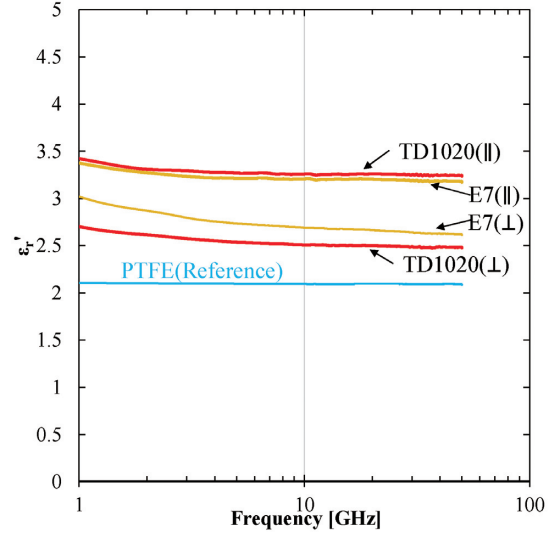


Fig.5 Frequency characteristics of relative permittivity ε_r' for dielectric anisotropy. (\parallel) denotes ε_r' in parallel component of respective LCs for TD1020 and E7, (\perp) denotes $\varepsilon_{r\perp}$ in perpendicular component for respective those of LCs.

measurement of S_{21} which is saturation state at applying 50 Vrms to the DUT coaxial line. In the case without applying any voltage to the DUT, a random orientation occurs because of no coat of the homogeneous alignment layer on the surface of the inner and the outer conductor contacting LCs in the DUT. The relative permittivity ε_{avr} in a random orientation of LCs is obtained from the measurement of S_{21} at applying 0 Vrms to the DUT coaxial line. The perpendicular component $\varepsilon_{r\perp}$ in dielectric anisotropy is expressed as equation (7) including the term for $\varepsilon_{r\parallel}$ and ε_{avr} ⁶.

$$\varepsilon_{r\perp} = \frac{3\varepsilon_{avr} - \varepsilon_{r\parallel}}{2} \quad (7)$$

The ε_r' of PTFE for the reference of coaxial line is almost independent of the frequency in the range from 1 GHz to 50 GHz, whereas the ε_r' of TD1020 and E7 decreases monotonously as frequency increases. Moreover, the different variation based on the dielectric anisotropy of the relative permittivity for TD1020 and E7 is observed in Figure 5.

The frequency dependence of loss tangent, i.e., the ratio of ε_r'' to ε_r' in complex permittivity is shown in Figure 6.

Frequency dependence of the loss tangent decreasing gradually toward higher frequency is observed. In addition, the loss tangent becomes a minimum in the region of 40 GHz.

It is suggested that these frequency dependence are derived from a dipole relaxation occurred in the lower frequency band less than 1 GHz. This is because it is presumed that the influence of dipole relaxation

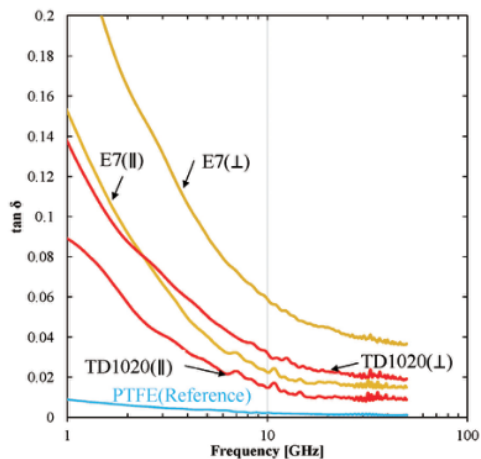


Fig.6 損失正接 $\tan \delta$ の周波数依存性。(//)はTD1020とE7のそれぞれのLCの平行成分における ϵ_r' 、(*)はTD1020とE7のそれぞれのLCの垂直成分における ϵ_r' を表す。

推測されるためである。

測定の結果、TD1020はE7と比較して、低損失正接と大きな誘電率異方性を持つIRSアンテナに対して優れた特性を示すことが明らかになった。

4.2 損失正接に及ぼすネマティックアイソトロピック転移温度の影響

アンテナの性能を向上させるために、損失正接の低減係数を考慮した。

温度⁷⁾の上昇に伴い損失正接が増加することに注目すると、液晶分子の熱振動が損失正接に影響を与えると推測される。

液晶状態が分子間相互作用と熱振動効果の競合によって示されると仮定すると、ネマティック等方性転移温度(T_{ni})が分子間相互作用の強さを表す指標の一つになると考えられる。

熱振動の強さが液晶の分子間相互作用の強さを超えている場合、ネマティック温度範囲の高温側で等方的な状態が現れる。液晶において熱振動の強さが分子間相互作用の強さを下回る場合、ネマティック温度範囲において低温側に結晶状態が現れる。強い分子間相互作用の場合、熱振動の強さが分子間相互作用の強さを超えるためには、より高い T_{ni} が必要となる。すなわち、分子間相互作用の影響が熱振動の影響に対して支配的である場合、結晶化温度は上昇する。

この観点から、単一液晶化合物の T_{ni} との結合や分子構造と比較すると、 T_{ni} が高い3環または4環液晶化合物は強い分子間相互作用を示すと推測される。一方、 T_{ni} の低い2環液晶化合物は弱い分子間相互作用を示す。すなわち、強い分子間相互作用を持つ3環または4環の液晶は、損失正接を減少させる効果があると予想される。

3または4環液晶における損失正接の低減効果を調べるために、5~20%の範囲で高い T_{ni} を示す単一化合物を添加した3種類の混合物を、2環液晶からなる65CB塩基性混合物に添加した。

混合物 65CB は 4-Cyano-4'-pentylbiphenyl (5CB, T_{ni} : 34.4° C) と 4-Cyano-4'-hexylbiphenyl (6CB, T_{ni} : 28.6° C) からなり、比率は 1 対 1 である。混合物1は、非極性化合物として4, 4'-Bis(trans-4-propyl cyclohexyl) biphenyl (HPPH, T_{ni} : 280° C) を5%添加したものであった。混合物2は、非極性化合物として4-エチル-4'-(トランス-4-プロピルシクロヘキシル)ピフェニル(HPP, T_{ni} :169° C)を65CBに1対9の割合で添加した。混合物3は、65CBに極性化合物として4-シアノ4'-ペンチル-p-テルフェニル(5CT, T_{ni} :240° C)を2対8の割合で添加した。

図7に示す損失正接の周波数依存性は、基本的な2環化合物混合物の65CBと、169° C以上の T_{ni} を持つ単一化合物を別々に含む3種類の混合物について、異なる曲線を示している。

損失正接を減少させる効果は、2環系で損失正接65CBに対して高い T_{ni} を持つ液晶化合物の添加によって観察されることが明らかになった。

高 T_{ni} 化合物を用いたこの基礎的な検討では、高 T_{ni} 液晶化合物を導入することで損失正接が減少するのに対し、2環液晶を用いると損失正接が増加する傾向があることが確認された。

高 T_{ni} 化合物の量を増やすことが可能であれば、損失正接を減らす効果は大きいだろうが、高 T_{ni} 液晶化合物の結晶化温度が高いため、化合物の量は限られている。

これらの観点から、低減損失正接の観点から、結晶化温度の抑制と低減損失正接のバランスをとるために、IRSアンテナに使用されるTD1020の化合物として3環系の量が増加する。

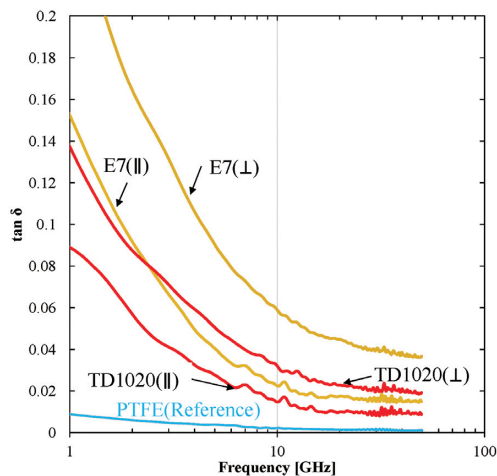


Fig.6 Frequency dependence of loss tangent $\tan\delta$. (\parallel) denotes ϵ_r' in parallel component of respective LCs for TD1020 and E7, (\perp) denotes ϵ_r' in perpendicular component of respective LCs for TD1020 and E7.

decreases gradually as frequency increases.

As the result of the measurements, it is revealed that TD1020 exhibits excellent properties for IRS antenna with low loss tangent and large dielectric anisotropy, when compared with E7.

4.2 Influence of Nematic-Isotropic Transition Temperature on Loss tangent

Factor for reduction of loss tangent was considered to improve the performance of antenna.

When we take notice of that loss tangent increases with increasing temperature⁷⁾, it is speculated that a thermal vibration of liquid crystalline molecule influences on a loss tangent.

When assuming that liquid crystal state is exhibited by the competition between molecular interactions and thermal vibration effects, it is considered that the nematic-isotropic transition temperature (T_{ni}) becomes one of indicator representing the strength of molecular interaction.

In the case of that the strength of thermal vibration is beyond the strength of molecular interactions in liquid crystals, an isotropic state appears at the side of a high temperature in nematic temperature range. In the case of that the strength of thermal vibration is below the strength of molecular interactions in liquid crystals, a crystal state appears at the side of a low temperature in nematic temperature range. In the case of the strong molecular interactions, a higher T_{ni} is required in order for the strength of thermal vibration to exceed the strength of molecular interactions. In other words, the crystallization temperature increases when the effect of molecular interaction is dominated against the effect of thermal vibration.

From this point of view, comparing to connections with T_{ni} and molecular structure for the single liquid crystal compound, it is speculated that 3 or 4-ring liquid crystal compounds with a high T_{ni} exhibits strong molecular interactions. On the other hands, 2-ring liquid crystal compounds having a low T_{ni} exhibit weak molecular interactions. In other words, 3 or 4-ring liquid crystals possessing strong molecular interactions are expected to have the effect of reducing loss tangent.

For probing the effectiveness of reducing loss tangent in 3 or 4 ring liquid crystals, 3 types of the mixture adding the single compound exhibiting high T_{ni} with amount ranging from 5 to 20% into 65CB basic mixture consisted of 2-ring liquid crystal is used.

Mixture 65CB is composed of 4-Cyano-4'-pentylbiphenyl (5CB, T_{ni} : 34.4°C) and 4-Cyano-4'-hexylbiphenyl (6CB, T_{ni} :28.6°C) with the ratio of 1 to 1. Mixture1 was that 5% of 4, 4'-Bis(trans-4-propylcyclohexyl) biphenyl (HPPH, T_{ni} : 280°C) as non-polar compound was added to 65CB. Mixture2 was that 4-Ethyl-4'-(trans-4-propylcyclohexyl) biphenyl (HPP, T_{ni} : 169°C) as non-polar compound was added to 65CB with the ratio of 1 to 9. Mixture 3 was adding 4-Cyano-4''-pentyl-p-terphenyl (5CT, T_{ni} : 240°C) as polar compound into 65CB with the ratio of 2 to 8.

Frequency dependence of loss tangent shown in Figure 7 exhibits the different curves for 65CB of the basic 2-ring compounds mixture and for 3 types of mixtures containing separately the single compound having T_{ni} more than 169 °C.

It is revealed that effects reducing loss tangent are observed by the addition of liquid crystal compounds having high T_{ni} against loss tangent of 65CB in 2 ring system.

In this fundamental examination using the high T_{ni} compounds, it is confirmed that the loss tangent is reduced by introducing a high T_{ni} liquid crystal compound, whereas using 2-ring liquid crystal tends to increase the loss tangent.

If it were possible to increase amounts of the high T_{ni} compounds, the effect reducing loss tangent would be significant, however amounts of the compounds are limited due to a high crystallization temperature of the high T_{ni} liquid crystal compounds.

From these points of view for the reducing loss tangent, amounts of 3 ring system are increased as compounds for TD1020 used to the IRS antenna in order to balance between the suppressing increase of crystallization temperature and the reducing loss tangent.

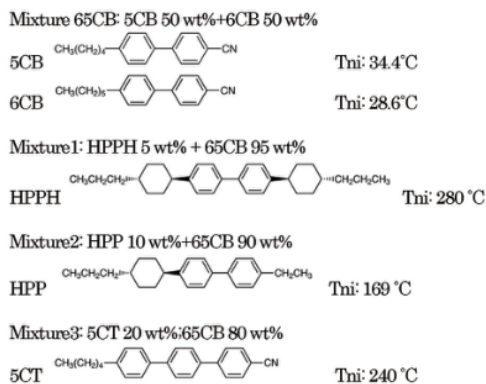
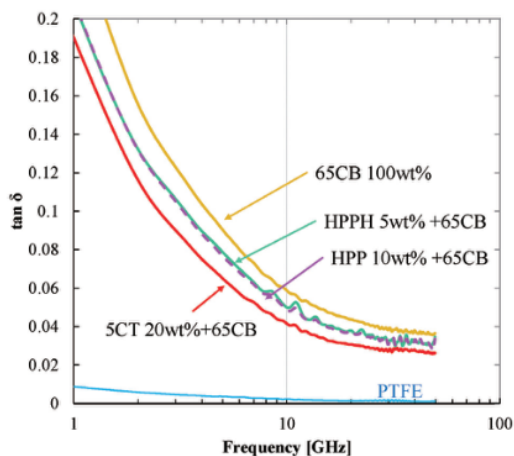


Fig.7 損失正接 $\tan \delta$ の周波数依存性を持つ 2 環化合物からなる 65CB の基本混合物に、高い T_{ni} を持つ単一化合物を添加した 3 種類の混合物との比較。

4.3 低周波LCの物理的特性 IRSアンテナの液晶の主題は、50 μm 以上の厚いLC層が必要であり、IRSアンテナの十分な位相変動を確保できるため、スイッチング時の減衰時間による位相シフト速度が極端に遅くなることである。

IRSアンテナは、低周波の外部電圧でギガヘルツ帯の比誘電率を調整する必要があるため、粘性などの液晶の物性や低周波での誘電異方性は、アンテナのビームステアリングに関する性能を決定する重要な特性である⁸⁾⁹⁾。

極性基がシアノ基である2環および3環化合物からなる組成のよく知られた液晶混合物E7は、回転粘度の増加をもたらし、スイッチングにおける遅い減衰時間を提供する。

粘度を下げるために、混合物における設計の概念を変える必要がある。極性化合物の量は、粘度の上昇を最小限に抑えるために、可能な限り減らすべきである。以上の説明から、損失正接の減少の観点から、損失正接の増加を引き起こす2つの環状化合物の低粘度を付加する代わりに、低損失正接を満たす3環を持つ非極性化合物の量を最大化することが必要である。この液晶組成の設計により、損失正接を増加させることなく、回転粘度を低下させることができる。

E7とTD1020の45GHzと1kHzの物性を表1に示す。IRSアンテナでは粘度の低下と損失正接が優先課題であるため、液晶のTD1020を選択した。一方、T_{ni}の高い4-Cyano4'-pentyl-p-terphenyl (5CT) 化合物 8 wt% と T_{ni}の低い n-alkylcyanobiphenyl 化合物 9 2 wt% を用いた E7 では、回転粘度と損失正接の両方が増加した。TD1020とE7の化合物量と極性の違いから、TD1020に用いたp-terphenylの3環非極性化合物は、回転粘度と損失正接に対して還元効果を示すことが明らかになった。

さらに、シアノ基を持たないプテルフェニル化合物では70 wt%を超えることで、TD1020の誘電異方性は0.61とわずかに生じ、E7の誘電異方性は1 kHzで12.24であった。セルギャップ50 μm のTD1020の立ち上がり時間は、印加電圧が12V_{rms}以上で1秒以下を示すため、立ち上がり時間と減衰時間からなる総スイッチング時間に対する立ち上がり時間の影響は、数秒の減衰時間と比較して無視できる値である。一方、減衰時間を改善するために、極性化合物の量を減らして回転粘度 γ_1 をE7の252 [mPa s]からTD1020の107 [mPa s]に下げると、

表1 45GHzおよび1kHzにおけるLCの物理的特性。

LC Mixture	45GHz					1kHz			V_{th}	γ_1	Δn	T _{ni}
	$\tan \delta_{\parallel}$	$\tan \delta_{\perp}$	ϵ_{\parallel}	ϵ_{\perp}	$\Delta \epsilon$	ϵ_{\parallel}	ϵ_{\perp}	$\Delta \epsilon$				
E7	0.0151	0.0364	3.18	2.62	0.56	14.4	4.2	12.24	0.82	252	0.21	58
TD1020	0.0095	0.0195	3.25	2.48	0.77	3.78	3.11	0.61	5	107	0.25	108.1

【機械翻訳コンテンツの著作権について】

当サイトに掲載されている原著論文の著作権は映像情報メディア学会に帰属します。原著論文および翻訳論文の無断使用は禁止します。引用の際には、必ず原著論文の書誌情報をご記載ください。詳細は映像情報メディア学会著作権規定をご覧ください。

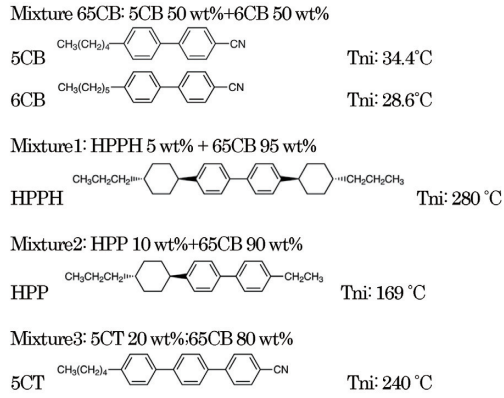
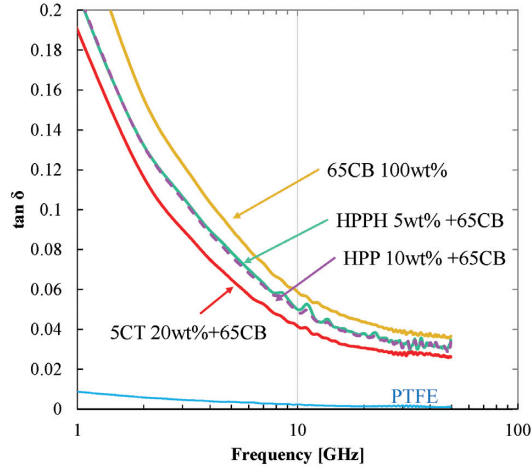


Fig.7 Comparison with 3 types of mixtures adding respective single compound having high Tni into the basic mixture of 65CB consisting of 2-ring compounds in frequency dependence of loss tangent $\tan \delta$.

4.3 Physical Properties for LCs in Low Frequency

The subject matter of liquid crystals for IRS antenna is to become extremely slow phase shifting speed on decay time in switching because of a necessary of thick LC layer over 50 μm ensuring sufficient phase variation in IRS antenna.

As IRS antenna requires an adjustment of relative permittivity in the gigahertz band with external voltage at the low frequency, physical properties of liquid crystals such as viscosity, and dielectric anisotropy at the low frequency are significant properties to determine the performance related to a beam steering of the antenna⁽⁸⁾⁹⁾.

Well-known liquid crystal mixture E7 of composition, which compose of 2-ring and 3-ring compounds having

polar groups being cyano groups, results in an increase of rotational viscosity providing for the slow decay time in the switching. To decrease the viscosity, concept of design in mixtures should be changed. The amounts of polar compounds should be reduced as possible to minimize an increase of viscosity. From a point of view for reduction of loss tangent with explanation above, it is necessary to maximize amount of non-polar compounds having 3-ring to satisfy a low loss tangent, instead of adding low viscosity of 2 ring compounds that cause an increase of loss tangent. By this design for liquid crystal compositions, the lowering rotational viscosity without the increase of loss tangent is attained.

Physical properties in 45 GHz and 1kHz for both E7 and TD1020 are listed in Table 1. As the lowering viscosity and loss tangent are priority issues for the IRS antenna, TD1020 of liquid crystals is selected.

3-ring of p-terphenyl compounds without a cyano group was used to achieve the low viscosity and a reduction of loss tangent in TD1020, whereas E7 using 8 wt% of 4-Cyano-4'-pentyl-p-terphenyl (5CT) compounds with a high Tni and 92 wt% of n-alkylcyanobiphenyl compounds with a low Tni causes the increasing both rotational viscosity and loss tangent. From a point of view with respect to the difference for amounts of compounds and for polarity of compounds between TD1020 and E7, it is revealed that 3-ring non-polar compounds of p-terphenyl used for TD1020 exhibit the effectiveness of reduction for the rotational viscosity and the loss tangent.

Moreover, by exceeding 70 wt% of amounts in the p-terphenyl compounds without a cyano group, a slight dielectric anisotropy of 0.61 for TD1020 arises in comparison with the dielectric anisotropy for E7 being 12.24 at 1 kHz. As the rise time for TD1020 with 50 μm of cell gap exhibits a 1 second or less at the applied voltage more than 12 Vrms, an influence of the rise time on a total switching time comprising the rise time and the decay time is a negligible value in the comparison with the decay time in a few seconds. On the other hand, in order to improve the decay time, the reduction of rotational viscosity γ_1 from 252 [mPa s] for E7 to 107

Table 1 Physical properties of LCs in 45 GHz and 1 kHz.

LC Mixture	45GHz					1kHz			V_{th}	γ_1	Δn	Tni
	$\tan\delta_{\parallel}$	$\tan\delta_{\perp}$	ϵ_{\parallel}	ϵ_{\perp}	$\Delta\epsilon$	ϵ_{\parallel}	ϵ_{\perp}	$\Delta\epsilon$				
E7	0.0151	0.0364	3.18	2.62	0.56	14.4	4.2	12.24	0.82	252	0.21	58
TD1020	0.0095	0.0195	3.25	2.48	0.77	3.78	3.11	0.61	5	107	0.25	108.1

減衰時間がE7の100 μ mのセルギャップで22秒からTD1020の同じセルギャップで10秒に短縮される。さらに、IRSアンテナのセルギャップ50 μ mで2.5秒の減衰時間が改善され、ビームステアリング動作に十分な位相変化を確保できることが確認された。

TD1020のシアノ基を持たない3-環を持つ非極性p-terphenyl化合物の量を増加させることにより、表1に示すように、TD1020の45GHz領域における0.0095という低い損失正接がE7のそれと比較して達成された。粘度の低下と損失正接が同時に達成されることが実証された。

5. Conclusion

ギガヘルツ地域のLCの評価方法を開発することが重要である。

この方法は、誘電率と損失正接の周波数依存性が、液晶を用いたDUTの同軸線とPTFEを用いた同軸線の移動波における伝搬の差から直接決定されることを特徴としている。

その結果、同軸線法を用いて、1~50GHzの広い周波数範囲における液晶の損失正接と比誘電率の両方の特性評価が達成された。

40GHz以上の周波数帯域では、損失正接を最小化する傾向が、40GHzの領域で動作するIRSアンテナの特性に適していることが明らかになった。

損失正接と液晶化合物の関係から、高いネマチック-等方性転移温度を示す3環または4環の液晶化合物は、損失正接が低い傾向があることが明らかになった。さらに、ネマチック-等方性転移温度が低い2環液晶化合物は逆の傾向がある。液晶の低損失接線を得るためには、液晶混合物に含まれる高損失接線を持つ2-リング化合物の量を減らすことが必要であることがわかった。

低周波およびギガヘルツ帯域の液晶混合物における組成の特性評価から、高T_{ni}を有する非極性3環化合物を最大量含む液晶混合物は、回転粘度と損失正接を同時に改善する方法として有用であることが判明した。

謝辞を述べる

本研究は、総務省の助成を受けて実施した(助成番号:JPJ000254)。

References

- 1) H. Maune, M. Jost, R. Reese, E. Polat, M. Nickel and R. Jakoby: "Microwave Liquid Crystal Technology", Crystals 8, 355 (2018)
- 2) Q. Wu, S. Zhang, B. Zheng, C. You, R. Zhang: "Intelligent Reflecting Surface-Aided Wireless Communications: A Tutorial", IEEE Trans. On Commun. Vol. 69, 5, pp.3313-3351 (May 2021)
- 3) Y. Cui, H. Sato, Y. Shibata, T. Ishinabe, H. Fujikake, Q. Chen: "A Low-Cost Structure for Reducing Reflection Loss in Intelligent Reflecting Surface of Liquid Crystal", IEEE Antennas Wireless Propag. Lett. Vol. 22.12 (Dec. 2023))
- 4) D.C. Zografopoulos, A. Ferraro and R. Beccherelli: "Liquid -Crystal High-Frequency Microwave Technology: Materials and Characterization", Adv. Mater. Technol. 4, 1800447 (2019)
- 5) X. Li, H. Sato, Y. Shibata, T. Ishinabe, H. Fujikake and Qiang Chen: "Development of beam Steerable Reflectarray With Liquid Crystal for Both E-Plane and H-Plane", IEEE Access, Vol. 10 pp.26177-26185 (2022)
- 6) T. Kamei, Y. Utsumi, H. Moritake, K. Toda and H. Suzuki: "Measurements of the Dielectric Properties of Nematic Liquid Crystals at 10 kHz to 40 GHz and Application to a Variable Delay Line", Electronics Commun. In Japan Part 2, Vol. 86, 8 (2008)
- 7) Y. Murakami, Y. Shibata, H. Sato, T. Ishinabe, Q. Chen and H. Fujikake: "Systematic Investigation of Molecular Structure of Nematic-phase Liquid Crystals for Reduction of Dielectric Loss in Microwave Control Applications", ITE Trans. On MTA Vol. 8, 4, pp-218-223 (2020)
- 8) E. Dumanis, R. Dickie, P. Baine, G. Perez-Palomino, R. Cahill, G. Goussetis, J. Encinar, M. Barba, S. Christie, N. Mitchell, M. Bain, G. Toso: "Nematic Liquid Crystals for Reconfigurable Millimeter Wavelength Antenna Technology", 7 th European conference on Antennas Propag.-Convened Sessions, pp.1791-1792 (2013)
- 9) J. Yang, P. Wang, S. Sun, Y. Li, Z. Yin and G. Deng: "A Novel Electronically Controlled Two-Dimensional Terahertz Beam-Scanning Reflectarray Antenna Based on Liquid Crystals", Frontiers in Physics, Vol. 8, Article 578045 (Oct. 2020)

[mPa s] for TD1020 by the decreasing amounts of polar compounds leads to an advancement of the decay time from 22 seconds at 100 μm of cell gap for E7 to 10 seconds for TD1020 at the same cell gap. In addition, the decay time at 2.5 seconds is improved with a 50 μm of cell gap in the IRS antenna, which is confirmed to ensure a sufficient phase change to operate a beam steering.

By increasing amount of non-polar p-terphenyl compounds having 3-ring without cyano groups on TD1020, the low loss tangent at 0.0095 for TD1020 in the region of 45GHz as shown in Table 1 is attained in comparison with that for E7. It is demonstrated that reducing viscosity and loss tangent are attained simultaneously.

5. Conclusion

It is important to develop the method for evaluation of LCs in gigahertz region.

The examined method is characterized with that frequency dependence of dielectric constant and loss tangent is determined directly from the difference of propagation in a travelling wave for the coaxial line of DUT using liquid crystal and for the coaxial line using PTFE.

Consequently, characterization of both loss tangent and relative permittivity for liquid crystals in a wide range of frequency from 1 to 50 GHz of have been achieved with the coaxial line method.

In the frequency band over 40 GHz, it is clarified that tendency of minimizing loss tangent is suitable for the properties in IRS antenna operating in the region of 40 GHz.

In relation between loss tangent and liquid crystal compounds, it has revealed that 3-ring or 4-ring liquid crystal compounds exhibiting a high nematic-isotropic transition temperature tend to be a low loss tangent. Furthermore, 2-ring liquid crystal compounds exhibiting a low nematic-isotropic transition temperature tend to be the contrary. It is found out that decrease of amounts of 2-ring compounds having a high loss tangent contained in liquid crystal mixtures is necessary for attaining low loss tangent of liquid crystals.

From characterization for composition on the liquid crystal mixtures in the low frequency and gigahertz band, it is found out that liquid crystal mixtures with the maximizing amount of non-polar 3-ring compounds having high T_{ni} are useful for method that improve simultaneously the rotational viscosity and the loss tangent.

Acknowledgements

This research has been supported by Ministry of Internal Affairs and Communications in Japan (Grant number: JPJ000254).

References

- 1) H. Maune, M. Jost, R. Reese, E. Polat, M. Nickel and R. Jakoby: "Microwave Liquid Crystal Technology", *Crystals* 8, 355 (2018)
- 2) Q. Wu, S. Zhang, B. Zheng, C. You, R. Zhang: "Intelligent Reflecting Surface-Aided Wireless Communications: A Tutorial", *IEEE Trans. On Commun.* Vol., 69, 5, pp.3313-3351 (May 2021)
- 3) Y. Cui, H. Sato, Y. Shibata, T. Ishinabe, H. Fujikake, Q. Chen: "A Low-Cost Structure for Reducing Reflection Loss in Intelligent Reflecting Surface of Liquid Crystal", *IEEE Antennas Wireless Propag. Lett.* Vol. 22.12 (Dec. 2023)
- 4) D.C. Zografopoulos, A. Ferraro and R. Beccherelli: "Liquid -Crystal High-Frequency Microwave Technology: Materials and Characterization", *Adv. Mater. Technol.* 4, 1800447 (2019)
- 5) X. Li, H. Sato, Y. Shibata, T. Ishinabe, H. Fujikake and Qiang Chen: "Development of beam Steerable Reflectarray With Liquid Crystal for Both E-Plane and H-Plane", *IEEE Access*, Vol. 10 pp.26177-26185 (2022)
- 6) T. Kamei, Y. Utsumi, H. Moritake, K. Toda and H. Suzuki: "Measurements of the Dielectric Properties of Nematic Liquid Crystals at 10 kHz to 40 GHz and Application to a Variable Delay Line", *Electronics Commun. In Japan Part 2*, Vol. 86, 8 (2008)
- 7) Y. Murakami, Y. Shibata, H. Sato, T. Ishinabe, Q. Chen and H. Fujikake: "Systematic Investigation of Molecular Structure of Nematic-phase Liquid Crystals for Reduction of Dielectric Loss in Microwave Control Applications", *ITE Trans. On MTA* Vol. 8, 4, pp-218-223 (2020)
- 8) E. Doumanis, R. Dickie, P. Baine, G. Perez-Palomino, R. Cahill, G. Goussetis, J. Encinar, M. Barba, S. Christie, N. Mitchell, M. Bain, G. Toso: "Nematic Liquid Crystals for Reconfigurable Millimeter Wavelength Antenna Technology", 7 th European conference on Antennas Propag.-Convened Sessions, pp.1791-1792 (2013)
- 9) J. Yang, P. Wang, S. Sun, Y. Li, Z. Yin and G. Deng: "A Novel Electronically Controlled Two-Dimensional Terahertz Beam-Scanning Reflectarray Antenna Based on Liquid Crystals", *Frontiers in Physics*, Vol. 8, Article 578045 (Oct. 2020)



Toru Fujisawa received his B.E. degree in electrical engineering from Tokyo Denki University in 1981 and joined DIC corporation (Previous Dainippon Ink & Chemicals). He engaged in research relating to fast switching liquid crystals such as ferroelectric liquid crystals, polymer network liquid crystals, nano phase separated liquid crystals for VA mode LCDs from 1984 to 2021. Since 2022, he has been engaged as academic researcher in Department of Communications Engineering, Graduate School of Engineering, Tohoku University, Sendai, Japan. His current research interest is adaption of liquid crystals to radio frequency fields from points of view on materials. He served as a Program Chair in Workshop on Electric Paper of International Display Workshops (IDW) from 2008 to 2018. He received the Outstanding Poster Paper Award from International Display Works (IDW) in 1998, 2001, and 2002, and the Best poster paper award from Society for Information Displays (SID) in 2000.



Hiroyasu Sato received the B.E. and M.E. degrees from Chuo University, Tokyo, Japan, in 1993 and 1995, respectively, and the D.E. degree from Tohoku University, Sendai, Japan, in 1998. He is currently an Assistant Professor with the Department of Communications Engineering, Tohoku University. His current research interests include the experimental study of electromagnetic waves, computational electromagnetics, antennas in plasma, antennas for plasma production, broadband antennas, wireless power transfer, and active/passive millimeter wave imaging. He is a member of the Institute of Electronics, Information and Communication Engineers (IEICE). He received the First Place of the Best Paper Award from the International Symposium on Antennas and Propagation (ISAP), in 2017. He is a member of the Institute of Electronics, Information and Communication Engineers (IEICE).



Wataru Ishikawa Received a B. E. degree from Tohoku University, Sendai, Japan, in 1979. He was a member of the Japan Science and Technology Agency from 2012 to 2017.



Hiraku Toshima received B.S. and M.S. the degrees Iwaki Meisei University, Iwaki, Japan, in 1991 and 1996. My Research area is studies about Natural products Organic Chemistry. The thesis titled "Deoxygenation and Stereoselective Reduction of Ulose Derivatives with Samarium Di-iodide." was written as master's thesis. In 1996-2006, as contract researcher from Suzuki Kougyou Co., Ltd. worked in Industrial Technology Institute, Miyagi Prefectural Government. My Research and Development was obtained as Patent about "New Recycled product on Manufacturing method by using wasted paper." Since 2022, I have worked at electronic engineering Lab in Tohoku Univ. Electronic Engineering Department from Co., Ltd. Focal Agency as dispatch researcher.



Masakazu Nakatani received his M.S. in Engineering from Nara Institute of Science and Technology (NAIST) in March 2010 and Ph.D. in Engineering from Nagaoka University of Technology in December 2020. From 2010-2016, he joined Clean Venture 21, a low-concentration photovoltaics venture company, as a researcher; from 2020-2022, he worked as a postdoctoral researcher at Osaka University, studying light control by cholesteric liquid crystals. In February 2023, he joined Graduate School of Engineering, Tohoku University as an Assistant Professor.



Takahiro Ishinabe received his B.S., M.S., and Ph. D. degrees in Electronic Engineering from Tohoku University, Sendai, Japan, in 1995, 1997, and 2000, respectively. From 2000 to 2002, he was a Research Fellow of the Japan Society for the Promotion of Science, and from 2003 to 2012, he was an Assistant Professor, and from 2013 to 2023, he was an Associate Professor in the Department of Electronics, Graduate School of Engineering, Tohoku University. Since 2023, he has been a Professor in the Department of Management Science and Technology, Graduate School of Engineering, Tohoku University. He has also been a Visiting Professor in the CREOL, The College of Optics and Photonics, University of Central Florida from 2010 to 2011. He has been performing research on advanced liquid crystal displays such as wide viewing angle LCD, reflective full-color LCD, field sequential color LCD, and flexible LCD. He is a fellow of the Society for Information Display.



Hideo Fujikake received M.E and Ph.D. degrees from Tohoku University, Japan, in 1985 and 2003, respectively. In 1985, he joined Japan Broadcasting Corporation (NHK) and he was with NHK Science and Technology Research Laboratories In 1988-2012. He was a Visiting Professor at Tokyo University of Science in 2006-2012. Since 2012, he has been a Professor at Department of Electronic Engineering, Tohoku University. His interest has been concerned with various functional liquid crystal devices. He received Best Paper Awards from Institute of Electronics, Information and Communication Engineers (IEICE) in 2001 and 2017, Best Paper Awards from Japanese Liquid Crystal Society (JLCS) in 2001 and 2015, Niwa-Takayanagi Best Paper Awards from Institute of Image Information and Television Engineers of Japan (ITE) in 2003 and 2009. He also obtained Achievement Awards from IEICE, ITE and JLCS in 2022, 2018 and 2017. He served as a General Chair in International Display Workshops (IDW) in 2021, a Japan Chapter Chair in IEEE Consumer Electronics Society in 2012-2014, and a Vice President of JLCS in 2015-2016. He is an IEICE fellow since 2015, ITE fellow since 2016, and JSAP (Japan Society of Applied Physics) fellow since 2019.



Qiang Chen received the B.E. degree from Xidian University, Xi'an, China, in 1986, the M.E. and D.E. degrees from Tohoku University, Sendai, Japan, in 1991 and 1994, respectively. He is currently Chair Professor of Electromagnetic Engineering Laboratory with the Department of Communications Engineering, Faculty of Engineering, Tohoku University. His primary research interests include antennas, microwave and millimeter wave, electromagnetic measurement and computational electromagnetics. He received the Best Paper Award and Zen-ichi Kiyasu Award from the Institute of Electronics, Information and Communication Engineers (IEICE). He served as the Chair of IEICE Technical Committee on Photonics-applied Electromagnetic Measurement from 2012 to 2014, the Chair of IEICE Technical Committee on Wireless Power Transfer from 2016 to 2018, the Chair of IEEE Antennas and Propagation Society Tokyo Chapter from 2017 to 2018, the Chair of IEICE Technical Committee on Antennas and Propagation from 2019 to 2021. IEICE Fellow.



Toru Fujisawa received his B.E. degree in electrical engineering from Tokyo Denki University in 1981 and joined DIC corporation (Previous Dainippon Ink & Chemicals). He engaged in research relating to fast switching liquid crystals such as ferroelectric liquid crystals, polymer network liquid crystals, nano phase separated liquid crystals for VA mode LCDs from 1984 to 2021. Since 2022, he has been engaged as academic researcher in Department of Communications Engineering, Graduate School of Engineering, Tohoku University, Sendai, Japan. His current research interest is adaption of liquid crystals to radio frequency fields from points of view on materials. He served as a Program Chair in Workshop on Electric Paper of International Display Workshops (IDW) from 2008 to 2018. He received the Outstanding Poster Paper Award from International Display Works (IDW) in 1998, 2001, and 2002, and the Best poster paper award from Society for Information Displays (SID) in 2000.



Hiroyasu Sato received the B.E. and M.E. degrees from Chuo University, Tokyo, Japan, in 1993 and 1995, respectively, and the D.E. degree from Tohoku University, Sendai, Japan, in 1998. He is currently an Assistant Professor with the Department of Communications Engineering, Tohoku University. His current research interests include the experimental study of electromagnetic waves, computational electromagnetics, antennas in plasma, antennas for plasma production, broadband antennas, wireless power transfer, and active/passive millimeter wave imaging. He is a member of the Institute of Electronics, Information and Communication Engineers (IEICE). He received the First Place of the Best Paper Award from the International Symposium on Antennas and Propagation (ISAP), in 2017. He is a member of the Institute of Electronics, Information and Communication Engineers (IEICE).



Wataru Ishikawa Received a B. E. degree from Tohoku University, Sendai, Japan, in 1979. He was a member of the Japan Science and Technology Agency from 2012 to 2017.



Hiraku Toshima received B.S. and M.S. the degrees Iwaki Meisei University, Iwaki, Japan, in 1991 and 1996. My Research area is studies about Natural products Organic Chemistry. The thesis titled "Deoxygenation and Stereoselective Reduction of Ulose Derivatives with Samarium Di-iodide." was written as master's thesis. In 1996-2006, as contract researcher from Suzuki Kougyou Co., Ltd. worked in Industrial Technology Institute, Miyagi Prefectural Government. My Research and Development was obtained as Patent about "New Recycled product on Manufacturing method by using wasted paper." Since 2022, I have worked at electronic engineering Lab in Tohoku Univ. Electronic Engineering Department from Co., Ltd. Focal Agency as dispatch researcher.



Masakazu Nakatani received his M.S. in Engineering from Nara Institute of Science and Technology (NAIST) in March 2010 and Ph.D. in Engineering from Nagaoka University of Technology in December 2020. From 2010-2016, he joined Clean Venture 21, a low-concentration photovoltaics venture company, as a researcher; from 2020-2022, he worked as a postdoctoral researcher at Osaka University, studying light control by cholesteric liquid crystals. In February 2023, he joined Graduate School of Engineering, Tohoku University as an Assistant Professor.



Takahiro Ishinabe received his B.S., M.S., and Ph. D. degrees in Electronic Engineering from Tohoku University, Sendai, Japan, in 1995, 1997, and 2000, respectively. From 2000 to 2002, he was a Research Fellow of the Japan Society for the Promotion of Science, and from 2003 to 2012, he was an Assistant Professor, and from 2013 to 2023, he was an Associate Professor in the Department of Electronics, Graduate School of Engineering, Tohoku University. Since 2023, he has been a Professor in the Department of Management Science and Technology, Graduate School of Engineering, Tohoku University. He has also been a Visiting Professor in the CREOL, The College of Optics and Photonics, University of Central Florida from 2010 to 2011. He has been performing research on advanced liquid crystal displays such as wide viewing angle LCD, reflective full-color LCD, field sequential color LCD, and flexible LCD. He is a fellow of the Society for Information Display.



Hideo Fujikake received M.E and Ph.D. degrees from Tohoku University, Japan, in 1985 and 2003, respectively. In 1985, he joined Japan Broadcasting Corporation (NHK) and he was with NHK Science and Technology Research Laboratories in 1988-2012. He was a Visiting Professor at Tokyo University of Science in 2006-2012. Since 2012, he has been a Professor at Department of Electronic Engineering, Tohoku University. His interest has been concerned with various functional liquid crystal devices. He received Best Paper Awards from Institute of Electronics, Information and Communication Engineers (IEICE) in 2001 and 2017, Best Paper Awards from Japanese Liquid Crystal Society (JLCS) in 2001 and 2015, Niwa-Takayanagi Best Paper Awards from Institute of Image Information and Television Engineers of Japan (ITE) in 2003 and 2009. He also obtained Achievement Awards from IEICE, ITE and JLCS in 2022, 2018 and 2017. He served as a General Chair in International Display Workshops (IDW) in 2021, a Japan Chapter Chair in IEEE Consumer Electronics Society in 2012-2014, and a Vice President of JLCS in 2015-2016. He is an IEICE fellow since 2015, ITE fellow since 2016, and JSAP (Japan Society of Applied Physics) fellow since 2019.



Qiang Chen received the B.E. degree from Xidian University, Xi'an, China, in 1986, the M.E. and D.E. degrees from Tohoku University, Sendai, Japan, in 1991 and 1994, respectively. He is currently Chair Professor of Electromagnetic Engineering Laboratory with the Department of Communications Engineering, Faculty of Engineering, Tohoku University. His primary research interests include antennas, microwave and millimeter wave, electromagnetic measurement and computational electromagnetics. He received the Best Paper Award and Zen-ichi Kiyasu Award from the Institute of Electronics, Information and Communication Engineers (IEICE). He served as the Chair of IEICE Technical Committee on Photonics-applied Electromagnetic Measurement from 2012 to 2014, the Chair of IEICE Technical Committee on Wireless Power Transfer from 2016 to 2018, the Chair of IEEE Antennas and Propagation Society Tokyo Chapter from 2017 to 2018, the Chair of IEICE Technical Committee on Antennas and Propagation from 2019 to 2021. IEICE Fellow.